JACC: CARDIOVASCULAR IMAGING VOL. 17, NO. 8, 2024
© 2024 THE AUTHORS. PUBLISHED BY ELSEVIER ON BEHALF OF THE AMERICAN COLLEGE OF CARDIOLOGY FOUNDATION. THIS IS AN OPEN ACCESS ARTICLE UNDER THE CC BY LICENSE (http://creativecommons.org/licenses/by/4.0/).

ORIGINAL RESEARCH

Development and Validation of a Quantitative Coronary CT Angiography Model for Diagnosis of Vessel-Specific Coronary Ischemia

Nick S. Nurmohamed, MD,[a,b,c] Ibrahim Danad, MD, PhD,[a,d] Ruurt A. Jukema, MD,[a] Ruben W. de Winter, MD,[a] Robin J. de Groot, BSc,[a] Roel S. Driessen, MD, PhD,[a] Michiel J. Bom, MD, PhD,[a] Pepijn van Diemen, MD,[a] Gianluca Pontone, MD, PhD,[e] Daniele Andreini, MD, PhD,[f] Hyuk-Jae Chang, MD, PhD,[g] Richard J. Katz, MD,[c] Erik S.G. Stroes, MD, PhD,[b] Hao Wang, MS,[h] Chung Chan, PhD,[h] Tami Crabtree, MS,[h] Melissa Aquino, MS,[h] James K. Min, MD,[h] James P. Earls, MD,[c,h] Jeroen J. Bax, MD, PhD,[i] Andrew D. Choi, MD,[c] Paul Knaapen, MD, PhD,[a] Alexander R. van Rosendael, MD, PhD,[i] the CREDENCE and PACIFIC-1 Investigators

ABSTRACT

BACKGROUND Noninvasive stress testing is commonly used for detection of coronary ischemia but possesses variable accuracy and may result in excessive health care costs.

OBJECTIVES This study aimed to derive and validate an artificial intelligence-guided quantitative coronary computed tomography angiography (AI-QCT) model for the diagnosis of coronary ischemia that integrates atherosclerosis and vascular morphology measures (AI-QCT$_{ISCHEMIA}$) and to evaluate its prognostic utility for major adverse cardiovascular events (MACE).

METHODS A post hoc analysis of the CREDENCE (Computed Tomographic Evaluation of Atherosclerotic Determinants of Myocardial Ischemia) and PACIFIC-1 (Comparison of Coronary Computed Tomography Angiography, Single Photon Emission Computed Tomography [SPECT], Positron Emission Tomography [PET], and Hybrid Imaging for Diagnosis of Ischemic Heart Disease Determined by Fractional Flow Reserve) studies was performed. In both studies, symptomatic patients with suspected stable coronary artery disease had prospectively undergone coronary computed tomography angiography (CTA), myocardial perfusion imaging (MPI), SPECT, or PET, fractional flow reserve by CT (FFR$_{CT}$), and invasive coronary angiography in conjunction with invasive FFR measurements. The AI-QCT$_{ISCHEMIA}$ model was developed in the derivation cohort of the CREDENCE study, and its diagnostic performance for coronary ischemia (FFR ≤0.80) was evaluated in the CREDENCE validation cohort and PACIFIC-1. Its prognostic value was investigated in PACIFIC-1.

RESULTS In CREDENCE validation (n = 305, age 64.4 ± 9.8 years, 210 [69%] male), the diagnostic performance by area under the receiver-operating characteristics curve (AUC) on per-patient level was 0.80 (95% CI: 0.75-0.85) for AI-QCT$_{ISCHEMIA}$, 0.69 (95% CI: 0.63-0.74; $P < 0.001$) for FFR$_{CT}$, and 0.65 (95% CI: 0.59-0.71; $P < 0.001$) for MPI. In PACIFIC-1 (n = 208, age 58.1 ± 8.7 years, 132 [63%] male), the AUCs were 0.85 (95% CI: 0.79-0.91) for AI-QCT$_{ISCHEMIA}$, 0.78 (95% CI: 0.72-0.84; $P = 0.037$) for FFR$_{CT}$, 0.89 (95% CI: 0.84-0.93; $P = 0.262$) for PET, and 0.72 (95% CI: 0.67-0.78; $P < 0.001$) for SPECT. Adjusted for clinical risk factors and coronary CTA-determined obstructive stenosis, a positive AI-QCT$_{ISCHEMIA}$ test was associated with aHR: 7.6 (95% CI: 1.2-47.0; $P = 0.030$) for MACE.

CONCLUSIONS This newly developed coronary CTA-based ischemia model using coronary atherosclerosis and vascular morphology characteristics accurately diagnoses coronary ischemia by invasive FFR and provides robust prognostic utility for MACE beyond presence of stenosis. (JACC Cardiovasc Imaging 2024;17:894-906) © 2024 The Authors. Published by Elsevier on behalf of the American College of Cardiology Foundation. This is an open access article under the CC BY license (http://creativecommons.org/licenses/by/4.0/).

ISSN 1936-878X https://doi.org/10.1016/j.jcmg.2024.01.007

Noninvasive functional testing strategies, such as nuclear myocardial perfusion imaging using positron emission tomography (PET) or single-photon emission computed tomography (SPECT) have been the cornerstone for the noninvasive detection of myocardial ischemia.[1-4] In the United States, SPECT imaging alone—as the dominant approach to coronary artery disease (CAD) imaging—may result in health care costs estimated at up to $2 billion and leads to a significant radiation burden.[5,6] In the United States and European guidelines, coronary computed tomography angiography (CTA) received a Class I indication for the use as a first-line test in patients with chest pain.[7-9] Atherosclerotic burden on coronary CTA is a strong and independent prognosticator of future cardiovascular events irrespective of the presence and extent of coronary ischemia.[10,11] Nevertheless, in daily clinical practice, the wealth of information provided by coronary CTA is not fully exploited because of time-consuming and labor-intensive nature of—as well as the interobserver variability observed with—a quantitative analysis.

Artificial intelligence-guided analysis of quantitative computed tomography (AI-QCT) has shown high diagnostic accuracy and enables rapid and objective quantitative assessment of adverse plaque characteristics including total plaque volume, plaque morphology, vessel volume, vessel involvement, and stenosis to guide risk stratification and therapy.[12-14] As atherosclerosis and vascular morphology form the cause for coronary ischemia, an important unanswered question remains: Could assessment of anatomic atherosclerosis, stenosis, and vascular morphology features accurately determine functional coronary ischemia? This substudy of the CREDENCE (Computed Tomographic Evaluation of Atherosclerotic Determinants of Myocardial Ischemia; NCT02173275) and PACIFIC-1 (Comparison of Coronary CT Angiography, SPECT, PET, and Hybrid Imaging for Diagnosis of Ischemic Heart Disease Determined by Fractional Flow Reserve; NCT01521468) trials[1,15] investigated the diagnostic performance and prognostic utility of a newly developed ischemia model ($AI\text{-}QCT_{ISCHEMIA}$) as first-line detection tool for coronary ischemia.

METHODS

STUDY POPULATION. The current study is a post hoc analysis of the CREDENCE study (n = 612) and the PACIFIC-1 study (n = 208).[1,15] CREDENCE included patients without known CAD scheduled to undergo clinically indicated nonemergent invasive coronary angiography (ICA), and patients were prospectively split in a derivation (n = 307) and a validation cohort (n = 305) based on inclusion date. Patients underwent coronary CTA and myocardial perfusion imaging (MPI)—SPECT, PET, or cardiac magnetic resonance (CMR)—and ICA with fractional flow reserve (FFR) measurements. PACIFIC-1 included patients without known CAD with an intermediate pretest likelihood and normal left ventricular ejection fraction, and all patients underwent coronary CTA, ICA with 3-vessel FFR, ^{99m}Tc-tetrofosmin SPECT, and [^{15}O]H_2O PET. Full inclusion and exclusion criteria, study design, as well as imaging techniques of both studies have been published previously.[1,15] Both studies were approved by the local ethics committee, with all patients visiting the study sites providing informed consent, and complied with the Declaration of Helsinki.

CORONARY CTA ACQUISITION. All coronary CTA scans were performed using single- or dual source computed tomography (CT) scanners with ≥64 detector rows (CREDENCE) or using a 256 detector row

ABBREVIATIONS AND ACRONYMS

AI-QCT = artificial intelligence-guided coronary computed tomography angiography

$AI\text{-}QCT_{ISCHEMIA}$ = ischemia model from AI-QCT

ASCVD = atherosclerotic cardiovascular disease

AUC = area under the receiving operating curve

CAD = coronary artery disease

CTA = computed tomography angiography

FFR = fractional flow reserve

FFR_{CT} = fractional flow reserve from coronary computed tomography angiography

MACE = major adverse cardiovascular events

MPI = myocardial perfusion imaging

PET = [^{15}O]H_2O position emission tomography

SPECT = ^{99m}Tc-tetrofosmin single photon emission computed tomography

From the [a]Department of Cardiology, Amsterdam UMC, Vrije Universiteit Amsterdam, Amsterdam, the Netherlands; [b]Department of Vascular Medicine, Amsterdam UMC, University of Amsterdam, Amsterdam, the Netherlands; [c]Division of Cardiology, The George Washington University School of Medicine, Washington, DC, USA; [d]Department of Cardiology, University Medical Center Utrecht, Utrecht, the Netherlands; [e]Department of Cardiovascular Imaging, Centro Cardiologico Monzino, IRCCS, Milan, Italy; [f]Division of University Cardiology, IRCCS Ospedale Galeazzi Sant'Ambrogio, Department of Biomedical and Clinical Sciences, University of Milan, Milan, Italy; [g]Division of Cardiology, Severance Cardiovascular Hospital and Severance Biomedical Science Institute, Yonsei University College of Medicine, Yonsei University Health System, Seoul, South Korea; [h]Cleerly Inc, Denver, Colorado, USA; and the [i]Department of Cardiology, Leiden University Medical Center, Leiden, the Netherlands.

Maros Ferencik, MD, served as Guest Editor for this paper.

The authors attest they are in compliance with human studies committees and animal welfare regulations of the authors' institutions and Food and Drug Administration guidelines, including patient consent where appropriate. For more information, visit the Author Center.

Manuscript received July 18, 2023; revised manuscript received November 30, 2023, accepted January 11, 2024.

CT scanner (PACIFIC-1) (Philips Brilliance iCT, Philips Healthcare) in accordance with the SCCT (Society of Cardiovascular Computed Tomography) guidelines, as described previously.[1,15-17]

AI-QCT$_{ISCHEMIA}$ FROM CORONARY CTA. Coronary CTA scans from both studies were analyzed using the previously described AI-QCT algorithm.[12,14] The quantitative coronary CTA evaluation was performed blinded to the clinical and outcome data. This Food and Drug Administration (FDA)-cleared software uses a series of validated convolutional neural networks (3-dimensional U-Net and Visual Geometry Group [VGG] network variants) for image-quality assessment, coronary segmentation and labeling, lumen-wall evaluation and vessel contour determination, and plaque characterization. The quantitative output of the AI-QCT algorithm includes the presence or absence of features of stenosis parameters such as percent diameter stenosis and area stenosis, number of severe stenosis >70%, and number of moderate stenosis 50% to 70%; atherosclerosis measurements such as noncalcified plaque volume, total plaque volume, and lesion length; vascular morphology features such as total vessel volume, total lumen volume, and vessel length; and diffuseness of atherosclerosis that includes a calculation of the sum of volumes and lengths across all involved segments.

Using these parameters, a model predicting ischemia was developed in the 307 patients in the derivation cohort of CREDENCE to predict a binary presence of ischemia defined as an invasive FFR ≤0.80 on a per-vessel basis. The model was developed using only the test results and invasive FFR measurements from the CREDENCE derivation cohort, blinded to the clinical, diagnostic, and outcome data. First, vessels with AI-QCT-determined stenosis ≤20% were automatically considered non-ischemic, vessels with AI-QCT-determined stenosis >80% were automatically considered ischemic. For the remaining vessels, a model predicting invasive FFR ≤0.80 was developed using 37 parameters from the AI-QCT algorithm.[18] Different machine-learning methods were tested for development of the model (logistic regression, random forest, extreme gradient boosting, and light gradient boosting), of which random forest achieved the most optimal internal performance in the derivation cohort (Supplemental Table 1). The final random forest model was constructed with hyperparameter tuning achieved via 10 repeated stratified 5-fold cross-validation. Bayesian hyperparameter optimization was used to maximize the average performance over the test sets across all random splits and folds.[19] The final model consisted of more than 1,000 decision trees, with a maximal depth of 7 layers in each tree. The AI-QCT$_{ISCHEMIA}$ threshold was determined to maximize the sum of sensitivity and specificity, with the constraint that vessel-territory-level specificity had to be above 0.80, resulting in a threshold of 0.31: ie, the probabilities from the AI-QCT$_{ISCHEMIA}$ random forest model were considered abnormal if ≥0.31. To determine the importance of the parameters used for prediction of ischemia in CREDENCE and PACIFIC-1, the top 5 absolute parameter importances were extracted per vessel. The sum of the absolute per-vessel importance was used to determine the overall importance per parameter. The importances were scaled from 0 to 1 to calculate relative importance and graphically displayed using the R package ggplot2.

FFR$_{CT}$ FROM CORONARY CTA. FFR$_{CT}$ measurements from coronary CTA scans were acquired as described earlier (HeartFlow [HeartFlow Holding, Inc] FFR$_{CT}$ version 2.7), in a blinded fashion.[1,16] Uninterpretable cases were rejected after an image-quality check by HeartFlow. In CREDENCE, FFR$_{CT}$ was measured at the most distal point in the segment with the maximal diameter stenosis. Vessels with ≤25% stenosis were considered normal. In PACIFIC-1, FFR$_{CT}$ values were extracted from the same position as the FFR wire, which was generally in the distal part of the vessel per PACIFIC-1 study protocol. For totally occluded coronary arteries, a value of 0.50 was assigned. For both studies, an FFR$_{CT}$ ≤0.80 was considered abnormal.

MPI ACQUISITION AND INTERPRETATION. In CREDENCE, MPI was performed using SPECT in 364 patients, using ^{99m}Tc and ^{201}Thallium/^{99m}Tc in 361, and 3 patients, respectively. A total of 42 patients underwent PET, using ^{82}Rubidium and ^{13N}-Ammonia in 35 and 13 patients, respectively. CMR was performed in 100 patients, predominantly using an adenosine stress protocol (n = 96). SPECT and PET MPIs were scored according to the 17-segment American Heart Association (AHA)/American College of Cardiology (ACC) model and summed stress scores (SSSs) were calculated per vessel territory. CMR imaging assessed rest and stress perfusion images according to 16 (excluding apex) of the 17-segment AHA/ACC model and graded as normal (0) and abnormal (1). Segmental scores were summed to per-vascular territory according to the standard segmentation. An SSS ≥1 was graded as abnormal.

In PACIFIC-1, patients underwent PET with 370 MBq of [^{15}O]H_2O during resting and adenosine-induced (140 μg/kg/min) hyperemic conditions.

Hyperemic myocardial blood flow (MBF) was calculated for all 3 major vascular territories. A hyperemic MBF ≤2.30 mL/min/g was considered abnormal. Furthermore, patients underwent SPECT with a 2-day stress-rest protocol with intravenous adenosine (140 μg/kg/min) for hyperemia and 370 to 550 MBq ^{99m}Tc-tetrofosmin as radiotracer. Summed difference scores (SDSs) were calculated from the 17-segment AHA/ACC model to account for vessel territory. An SDS ≥2 was considered abnormal.

INVASIVE CORONARY ANGIOGRAPHY AND FFR. In CREDENCE, ICA was performed in agreement with clinical indications and local standards. The major coronary arteries and side branches ≥2.0 mm with >40% or ≤90% lumen diameter stenosis underwent FFR measurement distal to the stenosis during intracoronary or intravenous adenosine infusion. Images were transferred to a blinded core laboratory for performance of quantitative coronary angiography and FFR reliability. In PACIFIC-1, ICA was performed following a standardized protocol with at least 2 orthogonal imaging directions per evaluated segment. Epicardial coronary vasodilation was induced using 0.2 mL of intracoronary nitroglycerin. Per PACIFIC-1 protocol, FFR measurements were performed in all 3 major coronary arteries in the distal part of the vessel, regardless of severity of stenosis, except for occluded or subtotally occluded (>90%) lesions. Intracoronary (150 μg) or intravenous (140 μg/kg/min) adenosine infusion was used to induce maximal coronary artery hyperemia. All images and FFR signals were interpreted by experienced interventional cardiologists blinded to the noninvasive imaging results. In both studies, FFR was calculated as the ratio of the mean distal intracoronary and the mean aortic pressure.

PACIFIC-1 PATIENT FOLLOW-UP. Follow-up data were collected during 2021 and 2022 using national registry databases, electronic medical records, and standardized telephone interviews,[20,21] between January and October 2022. Follow-up data were available in 204 of 208 patients (98%); 4 patients did not have follow-up available. Events were adjudicated in accordance with current guidelines.[8,21] For the follow-up analysis, the primary composite outcome was defined as all-cause mortality, nonfatal myocardial infarction, nonfatal stroke, and coronary revascularization (percutaneous coronary intervention or coronary artery bypass graft surgery). Early revascularization within 4 months as a consequence of the initial noninvasive imaging was excluded from this composite outcome.

STATISTICAL ANALYSIS. To assess the external performance of the AI-QCT$_{ISCHEMIA}$ algorithm, the performance of the different diagnostic modalities in the CREDENCE temporal validation cohort and the PACIFIC external validation cohort was reported, whereas internal validation in the CREDENCE derivation cohort was not reported. Vessels with missing invasive FFR values were excluded from the analysis. After exclusion of these vessels, the primary analysis was performed considering all missing test results positive (intention-to-diagnose). A secondary analysis was performed using multiple imputation of missing diagnostic test results. Finally, a tertiary analysis was performed excluding missing diagnostic results from the analysis.

All analyses were performed both on a per-patient as well as a per-vessel or vessel-territory basis. For the per-patient analysis, the most positive value for the particular diagnostic modality of the 3 vessels was used. The diagnostic performance (sensitivity, specificity, negative predictive value [NPV], positive predictive value [PPV] and accuracy) of the different ischemia modalities (AI-QCT$_{ISCHEMIA}$, FFR$_{CT}$, and MPI) for the test-specific thresholds was compared with an invasive FFR reference standard (FFR ≤0.80). For the area under the receiver-operating characteristic curve (AUC) analysis, the continuous diagnostic results were used. AUCs were compared with AI-QCT in a pairwise fashion, using a DeLong test. For the primary and tertiary analyses, sensitivity, specificity, NPV, PPV, and diagnostic accuracy were reported as simple frequencies as percentages with Wilson 95% CIs on a per-patient level and 2-sided bootstrapped 95% CIs with cluster sampling on a per-vessel level. AUCs were calculated using Mann-Whitney statistic with bootstrapped 95% CIs. The secondary analysis used multiple imputation to address missing data. First, missing test values were imputed in a data set with age, sex, body mass index, and total calcified plaque volume. The imputation was performed separately for the different diagnostic modalities. Given the multicenter design, site location was additionally used in the imputation model in CREDENCE. A linear regression imputation model was used to impute missing variables as continuous values for AI-QCT, FFR$_{CT}$, MPI, PET, and SPECT in the AUC analysis, whereas a discriminant model was used to impute missing variables as binary (positive/negative) for the analysis of the diagnostic performance measures with a binary threshold (sensitivity, specificity, NPV, PPV, and accuracy). A total of 25 imputed data sets were created for each modality. The resulting imputation data sets for the binary

JACC: CARDIOVASCULAR IMAGING, VOL. 17, NO. 8, 2024
AUGUST 2024:894-906

TABLE 1 Patient Characteristics in CREDENCE and PACIFIC-1

	CREDENCE Derivation (n = 307)	CREDENCE Validation (n = 305)	PACIFIC-1 (n = 208)
Age, y	64.4 ± 10.2	64.4 ± 9.8	58.1 ± 8.7
Male	218 (71)	210 (69)	132 (63)
Hypertension	197 (64)	197 (64)	96 (46)
Dyslipidemia	136 (44)	172 (56)	83 (40)
Diabetes mellitus type 2	95 (31)	91 (30)	33 (16)
Body mass index, kg/m^3	26.3 ± 4.2	26.3 ± 4.4	26.9 ± 3.7
Smoking history	148 (48)	144 (47)	99 (48)
Family history of CAD	60 (20)	60 (20)	107 (51)
Reason for referral			
Typical angina	110 (36)	123 (40)	71 (34)
Atypical angina	49 (16)	73 (24)	80 (38)
Aspecific chest pain	41 (13)	33 (11)	57 (27)
Asymptomatic	107 (35)	76 (25)	0 (0)
Aspirin use	186 (61)	176 (58)	182 (88)
Beta-blocker use	79 (26)	82 (27)	135 (65)
Use of calcium antagonists	86 (28)	103 (34)	61 (29)
Statin use	171 (56)	186 (61)	162 (78)
Use of long-acting nitrates	25 (8)	24 (8)	22 (11)
Follow-up duration, y	–	–	8.5 (7.9-9.3)

Values are mean ± SD, n (%), or median (IQR).
CAD = coronary artery disease.

diagnostic measures were reported using maximum likelihood estimation on a per-patient level while using a logistic regression model with generalized estimating equations (GEEs) on a per-vessel level to account for the multiple measures per patient. In the secondary analysis, AUCs were calculated using the Mann-Whitney statistic, whereas the 95% CIs for the AUCs, as well as for the diagnostic measures, were calculated using the estimates of the SE based on the between- and within-data sets variability.

In the PACIFIC-1 follow-up analysis, MACE-free survival was shown in a Kaplan-Meier analysis separately for the different diagnostic modalities, after which Cox regression models were constructed with the binary test results (positive/negative) from AI-QCT$_{ISCHEMIA}$, FFR$_{CT}$, PET, and SPECT as independent variables, respectively, and MACE as dependent variable. For the prognostic analysis, the most positive value for the particular diagnostic modality of the 3 vessels was used, whereas missing test values were imputed using the same multiple imputation approach as for the diagnostic analysis. Patients with missing follow-up data were excluded (n = 4). The Cox regression models were adjusted for age, sex, and cardiovascular risk as determined by the Systematic Coronary Risk Evaluation 2 (SCORE2) risk score and further for the presence of AI-QCT-determined obstructive stenosis (≥50%).

Data are presented as mean ± SD for normally distributed variables or median (IQR) for non-normally distributed data. Categorical variables are expressed as absolute numbers and percentages. The Shapiro-Wilk test was used to check the normality of the distribution. Per patient variables were compared between FFR ≤0.80 and nonischemic FFR >0.80 patient groups using the chi-squared test for binary variables, Wilcoxon Mann-Whitney U test for ordinal and non-normally distributed continuous variables, and the 2-sample Student's *t*-test for normally distributed continuous variables. Per-vessel variables were compared using logistic GEE for binary variables, GEE based on rank order[22] for ordinal and non-normally distributed continuous variables, and traditional GEE for normally distributed variables. All statistical analyses were performed using RStudio software version 4.0.3 (R Foundation) and SAS software version 9.4 (SAS Institute Inc).

RESULTS

The 307 patients from the CREDENCE derivation cohort used for development of the AI-QCT$_{ISCHEMIA}$ model had a mean age of 64.4 ± 10.2 years, and 218 (71%) were male. The 305 patients from the CREDENCE validation cohort had a mean age of 64.4 ± 9.8 years, and 210 (69%) were male, whereas the 208 patients from PACIFIC-1 had a mean age of 58.1 ± 8.7 years, with 132 (63%) male patients. Baseline characteristics of the cohorts are shown in Table 1. Diagnostic results for the different modalities for the CREDENCE validation cohort and PACIFIC-1 are shown in Table 2 and Table 3, respectively. In CREDENCE, 845 (97.4%), 745 (85.8%), and 856 (98.6%) vessels were interpretable for AI-QCT$_{ISCHEMIA}$, FFR$_{CT}$, and MPI, respectively (Supplemental Table 2). In PACIFIC-1, 581 (94.9%), 505 (82.5%), 600 (98.0%), and 599 (97.9%) vessels were interpretable for AI-QCT$_{ISCHEMIA}$, FFR$_{CT}$, SPECT, and PET, respectively.

AI-QCT$_{ISCHEMIA}$ MODEL FEATURES AND IMPORTANCE. The strongest contributors to the AI-QCT$_{ISCHEMIA}$ prediction model for vessel ischemia were percent diameter stenosis, percent area stenosis, number of severe stenosis, and minimal lumen diameter in both CREDENCE and PACIFIC-1 (Figure 1). Albeit with less importance, this list comprising the top 5 predictors per vessel also included several plaque-burden parameters beyond the number of stenosis, such as total plaque volume and percent atheroma volume.

TABLE 2 Per-Vessel Territory Parameters for Coronary CTA, FFR_{CT}, and MPI in CREDENCE

	Overall (N = 868)	FFR ≤0.80 (n = 229)	FFR >0.80 (n = 639)	*P* Value
AI-QCT				
Maximum diameter stenosis				<0.001
0%	16 (1.8)	0 (0.0)	16 (2.5)	
1%-29%	350 (40.3)	17 (7.4)	333 (52.1)	
30%-49%	236 (27.2)	49 (21.4)	187 (29.3)	
50%-69%	142 (16.4)	66 (28.8)	76 (11.9)	
70%-99%	82 (9.4)	62 (27.1)	20 (3.1)	
100%	42 (4.8)	35 (15.3)	7 (1.1)	
Percent atheroma volume	15.6 (8.9-24.8)	25.5 (16.8-33.1)	13.2 (7.3-20.4)	<0.001
Percent noncalcified plaque volume	10.6 (6.6-15.9)	14.8 (10.3-19.9)	9.3 (5.4-14.0)	<0.001
Percent calcified plaque volume	2.9 (0.7-8.2)	7.7 (1.8-15.6)	2.1 (0.4-5.9)	<0.001
Presence of low-density plaque	782 (90.1)	216 (94.3)	566 (88.6)	0.011
Interpretable vessels	845 (97.4)	220 (96.1)	625 (97.8)	0.893
$AI\text{-}QCT_{ISCHEMIA}$	0.12 (0.01-0.44)	0.65 (0.33-0.91)	0.06 (0.00-0.19)	<0.001
Positive $AI\text{-}QCT_{ISCHEMIA}$ ≥0.31	271 (32.1)	167 (75.9)	104 (16.6)	<0.001
FFR_{CT}				
Interpretable vessels	745 (85.8)	179 (78.2)	566 (88.6)	<0.001
FFR_{CT}	0.87 ± 0.18	0.73 ± 0.27	0.94 ± 0.09	<0.001
Positive FFR_{CT} ≤0.80	161 (21.6)	96 (53.6)	65 (11.5)	<0.001
MPI				
Interpretable vessels	856 (98.6)	229 (100.0)	627 (98.1)	0.999
SSS	0 (0-2)	1 (0-5)	0 (0-1)	<0.001
Positive SSS ≥1	343 (40.1)	134 (58.5)	209 (33.3)	<0.001

Values are n (%), median (IQR), or mean ± SD.

AI-QCT = artificial intelligence-guided quantitative coronary computed tomography angiography; CTA = computed tomography angiography; FFR = fractional flow reserve; FFR_{CT} = fractional flow reserve from coronary computed tomography; MPI = myocardial perfusion imaging; SSS = summed stress score.

DIAGNOSTIC PERFORMANCE OF $AI\text{-}QCT_{ISCHEMIA}$, FFR_{CT}, PET-CT, AND SPECT IN CREDENCE AND EXTERNAL PACIFIC-1 VALIDATION. In the primary intention-to-diagnose analysis of the CREDENCE validation cohort, on a per-patient basis, $AI\text{-}QCT_{ISCHEMIA}$ (AUC: 0.80 [95% CI: 0.75-0.85]) outperformed FFR_{CT} (AUC: 0.69 [95% CI: 0.63-0.74]; $P < 0.001$) and MPI (AUC: 0.65 [95% CI: 0.59-0.71]; $P < 0.001$) to diagnose coronary ischemia (Figure 2, Table 4). In the per-vessel territory analysis, $AI\text{-}QCT_{ISCHEMIA}$ (AUC: 0.86 [95% CI: 0.84-0.89]) also outperformed FFR_{CT} (AUC: 0.76 [95% CI: 0.72-0.80]; $P < 0.001$), and MPI (AUC: 0.65 [95% CI: 0.61-0.70]; $P < 0.001$) in diagnosing vessel-specific coronary ischemia (Table 4). In PACIFIC, $AI\text{-}QCT_{ISCHEMIA}$ (AUC: 0.85 [95% CI: 0.79-0.90]) outperformed FFR_{CT} (AUC: 0.78 [95% CI: 0.72-0.84]; $P = 0.037$) and SPECT (AUC: 0.72 [95% CI: 0.67-0.78]; $P < 0.001$) but not PET (AUC: 0.89 [95% CI: 0.84-0.93]; $P = 0.262$ (Table 4). Similar performance was found for the per-vessel territory analysis; $AI\text{-}QCT_{ISCHEMIA}$ achieved an AUC of 0.86 (95% CI: 0.83-0.89), similar to PET (AUC: 0.86 [95% CI: 0.81-0.90]; $P = 0.444$) (Table 4), numerically higher than FFR_{CT} (AUC: 0.83; [95% CI: 0.79-0.87]; $P = 0.062$), whereas outperforming SPECT (AUC: 0.68 [95% CI: 0.64-0.72]; $P < 0.001$). In the secondary (multiple imputation) and tertiary analysis (only interpretable vessels), performance of $AI\text{-}QCT_{ISCHEMIA}$ was superior to FFR_{CT} and MPI in CREDENCE (Supplemental Tables 3 and 4). In the secondary and tertiary analyses in PACIFIC-1, performance of $AI\text{-}QCT_{ISCHEMIA}$ was comparable with FFR_{CT} and PET, outperforming SPECT (Supplemental Tables 3 and 4).

PREDICTION OF FUTURE CARDIOVASCULAR EVENTS FROM PACIFIC-1. The mean follow-up time was 8.5 years (IQR: 7.9-9.3 years), during which the composite outcome occurred in 31 (15%) patients (Table 5). Patients with positive $AI\text{-}QCT_{ISCHEMIA}$, FFR_{CT}, or PET test—but not SPECT—had worse survival compared with patients with negative test results (Figure 2). Adjusted for clinical atherosclerotic cardiovascular disease (ASCVD) risk factors, the adjusted HR (aHR) for a cardiovascular event for a positive $AI\text{-}QCT_{ISCHEMIA}$ test was 7.2 (95% CI: 2.5-20.6; $P < 0.001$) (Table 6). Numerically lower values were observed for FFR_{CT} (aHR: 5.9 [95% CI: 1.8-19.9]; $P = 0.004$), and PET

TABLE 3 Per-Vessel Territory Parameters for Coronary CTA, FFR_{CT}, SPECT, and PET in PACIFIC-1

	Overall (N = 612)	FFR ≤0.80 (n = 165)	FFR >0.80 (n = 447)	*P* Value
AI-QCT				
Maximum diameter stenosis				<0.001
0%	108 (17.6)	8 (4.8)	100 (22.3)	
1%-29%	279 (45.6)	21 (12.7)	258 (57.8)	
30%-49%	64 (10.5)	23 (13.9)	41 (9.2)	
50%-69%	74 (12.1)	35 (21.2)	39 (8.7)	
70%-99%	69 (11.3)	60 (36.4)	9 (2.0)	
100%	18 (2.9)	18 (9.1)	0 (0.0)	
Percent atheroma volume	8.6 (1.5-22.4)	28.0 (15.5-41.3)	3.7 (0.9-13.6)	<0.001
Percent noncalcified plaque volume	4.5 (1.3-7.5)	13.6 (8.9-21.0)	2.8 (0.9-7.4)	<0.001
Percent calcified plaque volume	2.2 (0.0-6.7)	10.0 (3.8-22.7)	0.3 (0.0-4.0)	<0.001
Presence of low-density plaque	162 (26.5)	100 (61.0)	62 (13.9)	<0.001
Interpretable vessels	581 (94.9)	160 (97.0)	421 (94.2)	0.163
$AI\text{-}QCT_{ISCHEMIA}$	0.00 (0.00-0.45)	0.74 (0.31-0.95)	0.00 (0.00-0.04)	<0.001
Positive $AI\text{-}QCT_{ISCHEMIA}$ ≥0.31	165 (28.4)	120 (75.0)	45 (10.7)	<0.001
FFR_{CT}				
Interpretable vessels	505 (82.5)	135 (81.8)	370 (82.8)	0.782
FFR_{CT}	0.85 (0.74-0.90)	0.61 (0.50-0.74)	0.88 (0.84-0.91)	<0.001
Positive FFR-CT ≤0.80	175 (34.7)	122 (90.4)	53 (14.3)	<0.001
SPECT				
Interpretable vessels	600 (98.0)	160 (97.0)	440 (98.4)	0.247
SDS	0 (0-0)	0 (0-3)	0 (0-0)	<0.001
Positive SDS ≥2	90 (15.0)	63 (39.4)	27 (6.0)	<0.001
PET				
Interpretable vessels	599 (97.9)	161 (97.6)	438 (98.0)	0.754
hMBF	3.1 ± 1.3	1.9 ± 1.0	3.5 ± 1.2	<0.001
Positive hMBF ≤2.30	218 (36.4)	130 (80.7)	88 (20.1)	<0.001

Values are n (%), median (IQR), or mean ± SD.

hMBF = hyperemic myocardial blood flow; PET = $[^{15}O]H_2O$ position emission tomography; SDS = summed difference score; SPECT = ^{99m}Tc-tetrofosmin single-photon emission computed tomography; other abbreviations as in Table 2.

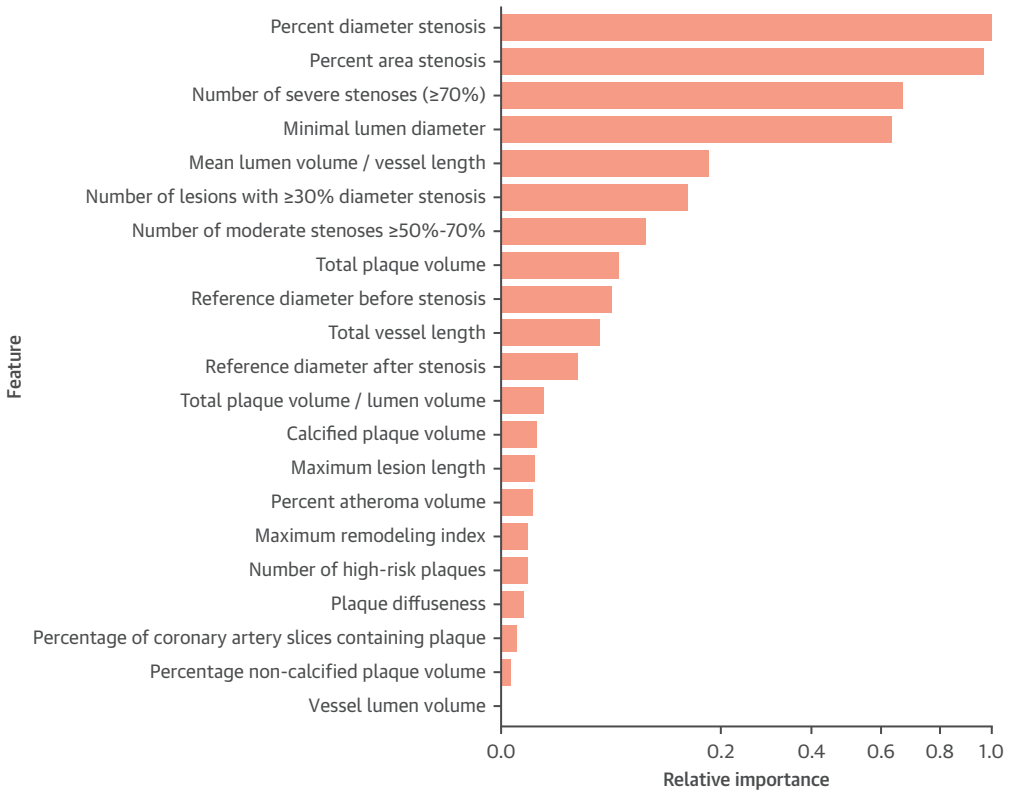
(aHR: 4.0 [95% CI: 1.6-10.3]; $P = 0.004$), and SPECT (aHR: 1.4 [95% CI: 0.6-3.0]; $P = 0.437$). In addition, when adjusted for the presence of obstructive stenosis, $AI\text{-}QCT_{ISCHEMIA}$ was the only modality to provide additional prognostic value beyond the presence of stenosis (aHR: 7.6 [95% CI: 1.2-47.0]; $P = 0.030$), in contrast to FFR_{CT} (aHR: 3.4 [95% CI: 0.9-13.1]; $P = 0.072$), PET (aHR: 2.3 [95% CI: 0.8-6.4]; $P = 0.101$), and SPECT (aHR: 0.8 [95% CI: 0.4-1.9]; $P = 0.691$).

DISCUSSION

Using 2 of the largest multimodality imaging studies with subjects undergoing evaluation by invasive FFR, we observed that next-generation AI-enabled coronary CTA analysis for stenosis, atherosclerosis, and vessel morphology characteristics effectively diagnosed hemodynamically significant CAD. The diagnostic performance of the coronary CTA-based model was similar to $[^{15}O]H_2O$ PET and superior to FFR_{CT} and SPECT in prediction of per-patient presence of reduced invasive FFR. Adjusted for clinical characteristics, a positive coronary CTA-based ischemia test put patients at a 7-fold higher risk of MACE during an 8-year follow-up and provided incremental prognostic utility over stenosis. Collectively, these data show that $AI\text{-}QCT_{ISCHEMIA}$ can predict presence of functional ischemia based on anatomic characteristics and support its use as an accurate diagnostic and prognostic approach to comprehensive coronary CTA-based assessment of atherosclerosis, stenosis, and ischemia (Central Illustration).

Previous data have shown that plaque phenotype identified on coronary CTA associated with coronary ischemia on invasive or noninvasive testing.[23-25] In a post hoc analysis from deFACTO (Determination of Fractional Flow Reserve by Anatomic Computed Tomographic Angiography), Park et al[23] found an association between adverse plaque characteristics (positive remodeling, low-attenuation plaque, and

FIGURE 1 **Feature Importance of AI-QCT$_{ISCHEMIA}$**



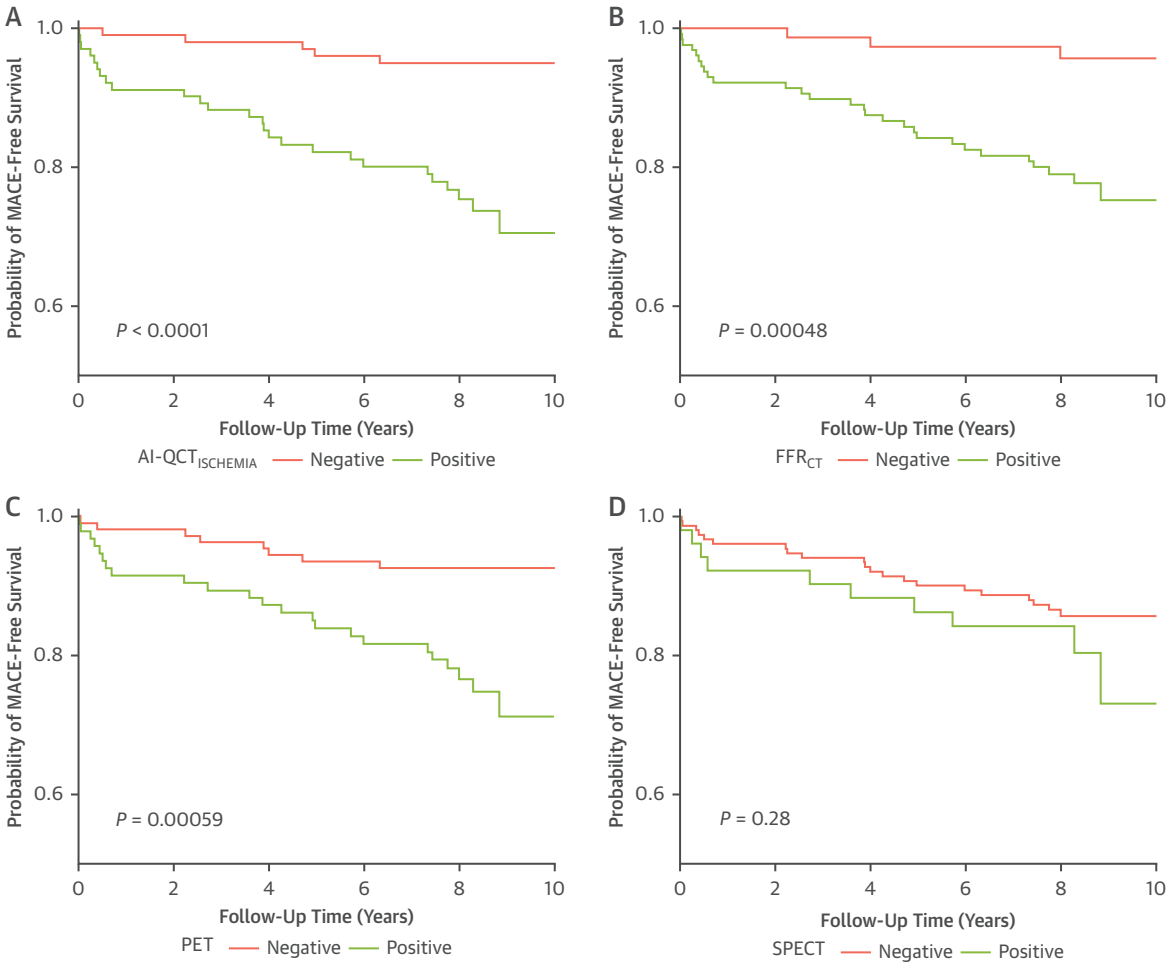
Shown is the relative importance of the parameters used in the random forest model, combined from CREDENCE validation and PACIFIC-1. The top 5 contributing parameters in the random forest model were summed per included vessel and scaled from 0 to 1 to provide an overview of the most important features of the model. AI-QCT = artificial intelligence-guided quantitative coronary CT angiography.

spotty calcification) and presence of vessel-specific ischemia determined by reduced invasive FFR in 407 coronary lesions. Gaur et al,[24] in a substudy of the NXT (Analysis of Coronary Blood Flow Using CT Angiography: Next Steps) trial, found that low-density noncalcified plaque and FFR$_{CT}$ provided diagnostic improvement over stenosis alone (AUC: 0.90 vs 0.71) for detecting ischemia defined by reduced invasive FFR. In another post hoc analysis from NXT,[25] it was shown that in lesions with a similar degree of luminal stenosis, lesions with FFR ≤0.80 had a significantly larger necrotic core compared with lesions with FFR >0.80. The aforementioned studies focused on only several individual quantitative and qualitative plaque characteristics that increase the risk of coronary ischemia. Recently, Lin et al[26] were the first to develop a machine-learning model derived from 19 plaque features derived from semiquantitative assessment that could predict coronary ischemia on invasive FFR and PET imaging effectively. In the current study, we performed external validation and long-term prognostic assessment of the newly developed ischemia model using PACIFIC-1. Using 37 AI-QCT-derived atherosclerotic plaque and stenosis features in a random forest model, this study illustrates the combined clinical potential of AI-QCT, including AI-QCT$_{ISCHEMIA}$, to readily and comprehensively identify patients and vessels with atherosclerosis, stenosis, and ischemia.

The most important parameters of the AI-QCT$_{ISCHEMIA}$ model in this study were related to the severe obstructive stenosis on coronary CTA, which has been shown to have important diagnostic and prognostic implications.[10] However, as illustrated by the fact that the AI-QCT$_{ISCHEMIA}$ model provided additional prognostic value over coronary CTA obstructive stenosis alone, there were several other

JACC: CARDIOVASCULAR IMAGING, VOL. 17, NO. 8, 2024
AUGUST 2024:894-906

FIGURE 2 MACE-Free Survival Stratified According to Diagnostic Modalities for Ischemia in PACIFIC-1



Shown are Kaplan-Meier curves comparing a positive and negative test of the different imaging modalities for the primary outcome of nonfatal myocardial infarction, nonfatal stroke, all-cause death, and coronary revascularization. AI-QCT = artificial intelligence-guided quantitative coronary CT angiography; FFR = fractional flow reserve; FFR_{CT} = fractional flow reserve from coronary computed tomography; MACE = major adverse cardiovascular events; PET = $[^{15}O]H_2O$ position emission tomography; SPECT = ^{99m}Tc-tetrofosmin single photon emission computed tomography.

important parameters predictive of coronary ischemia. Particularly, diffuseness of atherosclerotic plaque resembled by the number of obstructive and nonobstructive plaques as well as the length of the lesions proved important features in the model. This supports the hypothesis that diffuse, longer plaques—even without obstructive stenosis—can significantly affect myocardial blood flow caused by abnormal epicardial coronary arterial resistance.[27,28] In addition, the current study shows that plaque volume is inversely correlated to FFR values, and—in the model—plaque parameters, such as total plaque volume and percent atheroma volume, were predictors of ischemia, albeit less important than the stenosis and plaque diffuseness parameters. These findings are in line with previous published reports suggesting that large plaques, particularly low-density noncalcified plaques, can result in ischemia and reduced FFR through local inflammatory responses influencing vasodilatory capacity and thus coronary ischemia.[29,30] Finally, the characteristics observed in the current study—albeit with relatively limited importance—show significant overlap with previous studies regarding plaque-

TABLE 4 Performance of AI-QCT$_{ISCHEMIA}$, FFR$_{CT}$, and MPI for Detecting FFR ≤0.80, Primary Analysis

Trial/Test	Sensitivity	Specificity	PPV	NPV	Accuracy	AUC	AUC *P* Value
(A) CREDENCE: per patient (n = 305)							
AI-QCT$_{ISCHEMIA}$	85 (78-90)	56 (48-64)	69 (62-75)	76 (67-83)	72 (66-76)	0.80 (0.75-0.85)	Ref.
FFR$_{CT}$	63 (56-70)	66 (58-73)	68 (60-75)	61 (54-69)	64 (59-70)	0.69 (0.63-0.74)	<0.001
MPI	75 (68-81)	38 (30-46)	58 (51-65)	57 (47-67)	58 (52-63)	0.65 (0.59-0.71)	<0.001
(B) PACIFIC-1: per patient (n = 208)							
AI-QCT$_{ISCHEMIA}$	92 (85-96)	72 (63-79)	73 (64-80)	91 (83-95)	81 (75-86)	0.85 (0.79-0.90)	Ref.
FFR$_{CT}$	97 (91-99)	48 (39-57)	61 (53-68)	95 (86-98)	70 (64-76)	0.78 (0.72-0.84)	0.037
PET	87 (79-93)	84 (76-90)	82 (73-88)	89 (82-94)	86 (80-90)	0.89 (0.84-0.93)	0.262
SPECT	51 (41-61)	93 (88-96)	86 (76-93)	70 (62-77)	74 (68-80)	0.72 (0.67-0.78)	<0.001
(C) CREDENCE: per-vessel territory (n = 868)							
AI-QCT$_{ISCHEMIA}$	77 (71-82)	82 (78-85)	60 (54-66)	91 (88-93)	80 (77-83)	0.86 (0.84-0.89)	Ref.
FFR$_{CT}$	64 (58-70)	78 (75-82)	51 (45-58)	86 (83-89)	75 (72-78)	0.76 (0.72-0.80)	<0.001
MPI	59 (52-65)	65 (61-69)	38 (32-43)	82 (78-85)	64 (60-67)	0.65 (0.61-0.70)	<0.001
(D) PACIFIC-1: per-vessel territory (n = 612)							
AI-QCT$_{ISCHEMIA}$	76 (68-83)	84 (80-88)	64 (56-71)	90 (87-93)	82 (78-85)	0.86 (0.83-0.89)	Ref.
FFR$_{CT}$	92 (87-96)	71 (66-76)	54 (46-61)	96 (93-98)	77 (73-80)	0.83 (0.79-0.87)	0.062
PET	81 (74-88)	78 (73-84)	58 (50-66)	92 (88-95)	79 (75-83)	0.86 (0.81-0.90)	0.444
SPECT	41 (32-50)	92 (89-95)	67 (57-77)	81 (76-85)	79 (74-83)	0.68 (0.64-0.72)	<0.001

Shown are the performance metrics with 95% CIs of different diagnostic modalities for myocardial ischemia to predict presence of a reduced invasive FFR ≤0.80 on a per-patient basis (A,B) and a per-vessel territory basis (C,D) for both the CREDENCE (A and C) as well as PACIFIC-1 study (B and D). Results are from the primary (intention-to-diagnose) analysis; missing values were imputed as positive. Sensitivity, specificity, PPV, and NPV and accuracy are shown as proportions in %.

NPV = negative predictive value; PET = [^{15}O]H_2O position emission tomography; PPV = positive predictive value; SPECT = ^{99m}Tc-tetrofosmin single photon emission computed tomography; other abbreviations as in Tables 2 and 3.

based ischemia prediction,[23-25] underlining that there are other coronary CTA-derived factors than only the percent diameter stenosis that determine coronary ischemia, stressing the need for a comprehensive approach for quantification of plaque and vessel morphology from the entire coronary artery.

The 8-year follow-up data showed that patients with ischemia-positive vessels, as defined by AI-QCT$_{ISCHEMIA}$, had worse MACE-free survival than patients with no positive vessels independent from clinical characteristics and presence of obstructive stenosis, in a manner more potent than FFR$_{CT}$, PET, and SPECT. It is important to consider that patients in the PACIFIC-1 study underwent revascularization upon an FFR-significant lesion. Despite revascularization, the presence of a positive ischemia test at baseline illustrated major discriminative power for MACE during follow-up. Although speculative, these data suggest that quantitative characteristics of coronary atherosclerosis, such as plaque diffuseness included in the AI-QCT$_{ISCHEMIA}$ model, may ultimately determine prognosis in addition to coronary stenosis or ischemia that lead to symptoms of angina. This is in line with the results from ISCHEMIA (Initial Invasive or Conservative Strategy for Stable Coronary Disease), illustrating that not the severity of ischemia itself but the extent of atherosclerotic CAD predicted future ASCVD events.[11]

The observation that coronary CTA-based ischemia assessment outperformed myocardial perfusion imaging (except for [^{15}O]H_2O PET) in this study challenges the status quo of detection of ischemia by myocardial perfusion imaging. An additional advantage of coronary CTA over nuclear imaging techniques is the possibility to evaluate plaque burden and stenosis for prognostication.[13,14] For clinical implementation of coronary CTA for diagnosis of ischemia, an important advantage of AI-QCT$_{ISCHEMIA}$ over FFR$_{CT}$ was illustrated in both studies by its superior performance in the primary intention-to-diagnose analysis resembling clinical practice, driven by a combined

TABLE 5 Incidence of Major Adverse Cardiovascular Events During PACIFIC-1 Follow-Up (N = 204)

	Patients With Follow-Up Data Available
Major adverse cardiovascular event[a]	31 (15.2)
Nonfatal myocardial infarction	9 (4.4)
Nonfatal stroke	4 (2.0)
All-cause death	7 (3.4)
Coronary revascularization	11 (5.4)

Values are n (%). [a]Only first cardiovascular events are shown.

JACC: CARDIOVASCULAR IMAGING, VOL. 17, NO. 8, 2024
AUGUST 2024:894-906

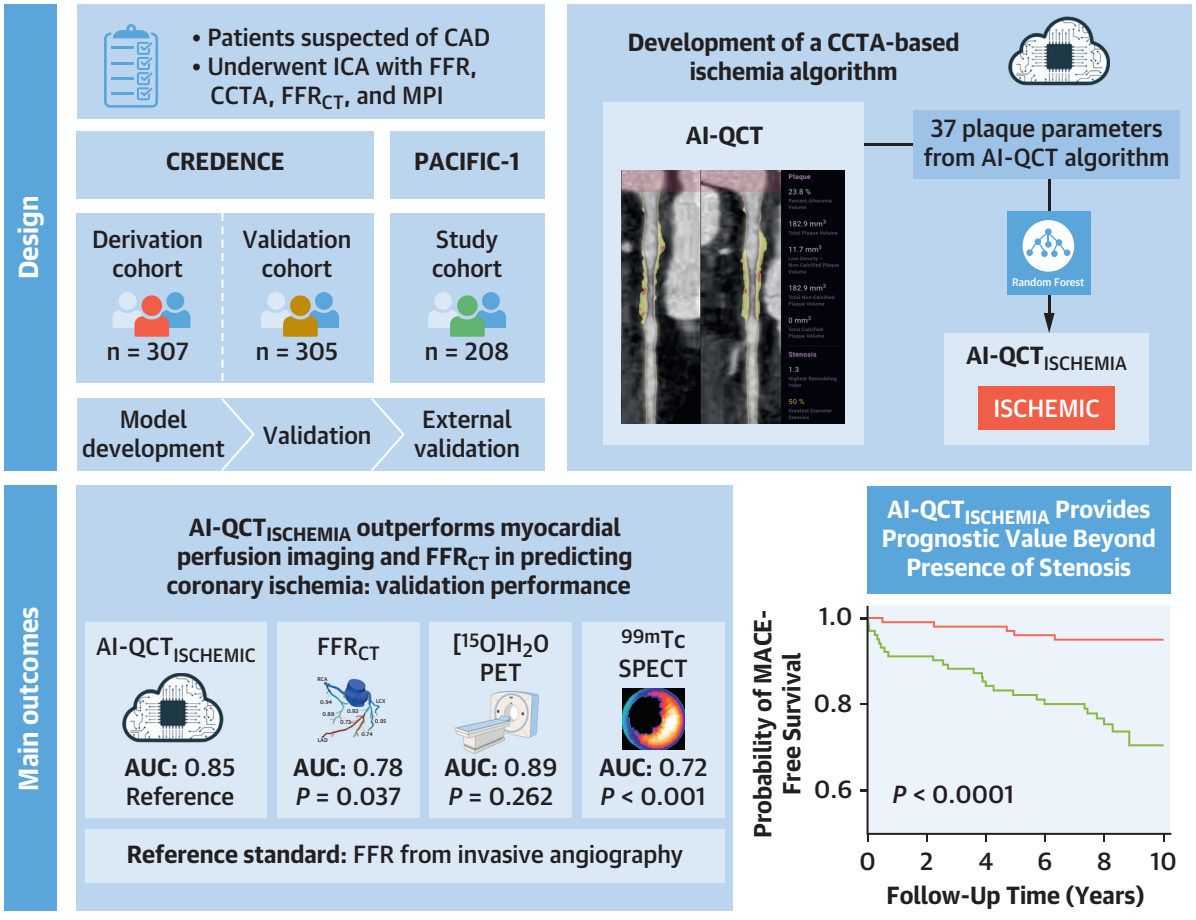
TABLE 6 Multivariable Cox Regression Using the Different Diagnostic Modalities for Prediction of the Primary MACE Outcome in PACIFIC-1

Test	Unadjusted HR (95% CI)	*P* Value	Adjusted for RF aHR (95% CI)	*P* Value	Adjusted for RF and ≥50% Stenosis aHR (95% CI)	*P* Value
AI-QCT$_{ISCHEMIA}$	6.0 (2.3-15.7)	<0.001	7.2 (2.5-20.6)	<0.001	7.6 (1.2-47.0)	0.030
FFR$_{CT}$	6.4 (1.9-20.9)	0.002	5.9 (1.8-19.9)	0.004	3.4 (0.9-13.1)	0.072
PET	3.7 (1.7-8.3)	0.001	4.0 (1.6-10.3)	0.004	2.3 (0.8-6.4)	0.101
SPECT	1.5 (0.7-3.2)	0.282	1.4 (0.6-3.0)	0.437	0.8 (0.4-1.9)	0.691

Shown are unadjusted adjusted HRs and *P* values for a positive test compared with a negative test from multivariable Cox regression models adjusted for SCORE2 risk for every diagnostic modality separately. In addition, models were further adjusted for presence of obstructive stenosis (≥50%). The primary outcome variable was a composite of nonfatal myocardial infarction, nonfatal stroke, all-cause death, and coronary revascularization.

aHR = adjusted HR; RF = clinical risk factors; SCORE2 = Systematic Coronary Risk Evaluation 2; other abbreviations as in Tables 2 and 3.

CENTRAL ILLUSTRATION Development, Diagnostic Accuracy, and Prognostic Value of a Quantitative Coronary CTA Model for Diagnosis of Vessel-Specific Coronary Ischemia



Nurmohamed NS, et al. JACC Cardiovasc Imaging. 2024;17(8):894-906.

AI-QCT = artificial intelligence-guided quantitative coronary computed tomography angiography; CT = computed tomography; CTA = computed tomography angiography; FFR = fractional flow reserve; FFR$_{CT}$ = fractional flow reserve from coronary computed tomography; MACE = major adverse cardiovascular events; MPI = myocardial perfusion imaging; PET = position emission tomography; SPECT = single-photon emission computed tomography.

4-fold lower vessel rejection rate (3.6% vs 15.5%), limiting the need for additional (non)invasive imaging in case of a nondiagnostic vessel. However, in the secondary analysis (imputation), and tertiary analysis restricted to interpretable vessels, overall performance of the diagnostic modalities improved and FFR_{CT} (AUC: ~0.90) performed largely similar to AI-$QCT_{ISCHEMIA}$ (AUC: ~0.90). This is in line with previous studies from PACIFIC-1,[16] NXT,[31] deFACTO,[32] and DISCOVER-FLOW (Diagnosis of Ischemia-Causing Stenoses Obtained Via Noninvasive Fractional Flow Reserve)[33] and suggests, when interpretable, a similar discriminatory performance of AI-$QCT_{ISCHEMIA}$ and FFR_{CT} for detecting vessel-specific ischemia defined by invasive FFR.

Altogether, quantitative coronary CTA analysis may enable an all-embracing approach to early prevention, determination of ischemia to guide symptom management, appropriate evaluation for revascularization, and accurate prognostication. The introduction of photon-counting CT scanners may even further increase the utility of coronary CTA in such an approach.[34]

STUDY LIMITATIONS. Performance of the different diagnostic modalities was generally lower in CREDENCE than PACIFIC-1, which may relate to a higher prevalence and burden of CAD in CREDENCE compared with PACIFIC-1 as well as differences in FFR measurement. In CREDENCE, invasive FFR was measured distal in the segment with maximal obstructive stenosis, whereas, per PACIFIC-1 protocol, FFR was measured distal in the vessel. Despite the availability of long-term follow-up data, the relatively small sample size in PACIFIC-1 limited power for the retrospective outcome analysis. In the quantitative plaque analysis, the amount of low-density plaque volume was relatively small, in contrast to other analyses using the same study population but a different algorithm for plaque quantification.[26] Although AI-QCT has been validated against ICA, intravascular ultrasound, optical coherence tomography, near infrared spectroscopy, and expert readers,[12-14,35,36] these differences among algorithms are important to consider when comparing studies analyzed using different quantitative coronary CTA algorithms. Finally, further larger prospective multicenter studies are needed to evaluate the real-world performance of AI-$QCT_{ISCHEMIA}$ across different populations, also with a lower prevalence of disease.

CONCLUSIONS

An ischemia model based on AI-guided quantitative coronary CTA parameters can effectively diagnose coronary ischemia as determined by invasive FFR and provides important prognostic value for future cardiovascular events. By its inclusion, coronary CTA may serve as an accurate all-inclusive, multiparametric approach to define coronary artery atherosclerosis, stenosis, and ischemia.

FUNDING SUPPORT AND AUTHOR DISCLOSURES

This project has been supported by the Foundation "De Drie Lichten" in the Netherlands. Dr Nurmohamed has received grants from the Dutch Heart Foundation (Dekker 03-007-2023-0068) and grants from the European Atherosclerosis Society (2023); and is co-founder of Lipid Tools. Mr Wang, Dr Chan, Ms Crabtree, Ms Aquino, Dr Min, and Dr Earls are employees of Cleerly Inc. Dr Choi has received grant support from GW Heart and Vascular Institute; equity in Cleerly, Inc; and has received consulting fees from Siemens Healthineers. Dr Knaapen has received research grants from HeartFlow, Inc. All other authors have reported that they have no relationships relevant to the contents of this paper to disclose.

ADDRESS FOR CORRESPONDENCE: Dr Nick S. Nurmohamed, Departments of Cardiology and Vascular Medicine, Amsterdam University Medical Centers-University of Amsterdam, Meibergdreef 9, 1105 AZ, Amsterdam, the Netherlands. E-mail: n.s.nurmohamed@amsterdamumc.nl.

PERSPECTIVES

COMPETENCY IN MEDICAL KNOWLEDGE: AI-QCT analysis can predict vessel-specific coronary ischemia accurately. Integrating coronary atherosclerosis and vascular morphology characteristics, the newly developed AI-$QCT_{ISCHEMIA}$ model diagnosed coronary ischemia accurately by invasive FFR and outperformed traditional myocardial perfusion imaging.

TRANSLATIONAL OUTLOOK: This newly developed coronary CTA-based ischemia model can be used to assess coronary ischemia accurately and noninvasively, enabling coronary CTA to become a comprehensive assessment of atherosclerosis, stenosis, and coronary ischemia. The ischemia model provides important prognostic value for future cardiovascular events.

JACC: CARDIOVASCULAR IMAGING, VOL. 17, NO. 8, 2024
AUGUST 2024:894–906

REFERENCES

1. Stuijfzand WJ, van Rosendael AR, Lin FY, et al. Stress myocardial perfusion imaging vs coronary computed tomographic angiography for diagnosis of invasive vessel-specific coronary physiology: predictive modeling results from the Computed Tomographic Evaluation of Atherosclerotic Determinants of Myocardial Ischemia (CREDENCE) trial. *JAMA Cardiol*. 2020;5:1338–1348.

2. Gould KL. Does coronary flow trump coronary anatomy? *JACC Cardiovasc Imaging*. 2009;2:1009–1023.

3. Tonino PAL, Fearon WF, De Bruyne B, et al. Angiographic versus functional severity of coronary artery stenoses in the fame study. fractional flow reserve versus angiography in multivessel evaluation. *J Am Coll Cardiol*. 2010;55:2816–2821.

4. Pijls NHJ, Fearon WF, Tonino PAL, et al. Fractional flow reserve versus angiography for guiding percutaneous coronary intervention in patients with multivessel coronary artery disease: 2-Year follow-up of the FAME (fractional flow reserve versus angiography for multivessel evaluation) study. *J Am Coll Cardiol*. 2010;56:177–184.

5. Einstein AJ, Berman DS, Min JK, et al. Patient-centered imaging: shared decision making for cardiac imaging procedures with exposure to ionizing radiation. *J Am Coll Cardiol*. 2014;63:1480–1489.

6. Schwartz AL, Landon BE, Elshaug AG, Chernew ME, McWilliams JM. Measuring low-value care in Medicare. *JAMA Intern Med*. 2014;174:1067–1076.

7. Gulati M, Levy PD, Mukherjee D, et al. 2021 AHA/ACC/ASE/CHEST/SAEM/SCCT/SCMR Guideline for the evaluation and diagnosis of chest pain: a report of the American College of Cardiology/American Heart Association Joint Committee on Clinical Practice Guidelines. *J Am Coll Cardiol*. 2021;78:e187–e285.

8. Knuuti J, Wijns W, Saraste A, et al. 2019 ESC guidelines for the diagnosis and management of chronic coronary syndromes. *Eur Heart J*. 2020;41:407–477.

9. The SCOT-Heart Investigators. Coronary CT angiography and 5-year risk of myocardial infarction. *N Engl J Med*. 2018;379:924–933.

10. Min JK, Dunning A, Lin FY, et al. Age- and sex-related differences in all-cause mortality risk based on coronary computed tomography angiography findings results from the International Multicenter CONFIRM (Coronary CT Angiography Evaluation for Clinical Outcomes: an international multicenter registry of 23,854 patients without know coronary artery disease. *J Am Coll Cardiol*. 2011;58:849–860.

11. Reynolds HR, Shaw LJ, Min JK, et al. Outcomes in the ISCHEMIA trial based on coronary artery disease and ischemia severity. *Circulation*. 2021;144:1024–1038.

12. Choi AD, Marques H, Kumar V, et al. CT Evaluation by Artificial Intelligence for Atherosclerosis, Stenosis and Vascular Morphology (CLARIFY): a multi-center, international study. *J Cardiovasc Comput Tomogr*. 2021;15:470–476.

13. Nurmohamed NS, Bom MJ, Jukema RA, et al. AI-guided quantitative plaque staging predicts long-term cardiovascular outcomes in patients at risk for atherosclerotic CVD. *JACC Cardiovasc Imaging*. 2024;17(3):269–280.

14. Griffin WF, Choi AD, Riess JS, et al. AI evaluation of stenosis on coronary CTA, comparison with quantitative coronary angiography and fractional flow reserve: a CREDENCE trial substudy. *JACC Cardiovasc Imaging*. 2023;16:193–205.

15. Danad I, Raijmakers PG, Driessen RS, et al. Comparison of coronary CT angiography, SPECT, PET, and hybrid imaging for diagnosis of ischemic heart disease determined by fractional flow reserve. *JAMA Cardiol*. 2017;2:1100–1107.

16. Driessen RS, Danad I, Stuijfzand WJ, et al. Comparison of coronary computed tomography angiography, fractional flow reserve, and perfusion imaging for ischemia diagnosis. *J Am Coll Cardiol*. 2019;73:161–173.

17. Leipsic J, Abbara S, Achenbach S, et al. SCCT guidelines for the interpretation and reporting of coronary CT angiography: a report of the Society of Cardiovascular Computed Tomography Guidelines Committee. *J Cardiovasc Comput Tomogr*. 2014;8:342–358.

18. Niculescu-Mizil A, Caruana R. Predicting good probabilities with supervised learning. Paper presented at: ICML 2005: Proceedings of the 22nd International Conference on Machine Learning; August 7-11, 2005; Bonn, Germany.

19. Wu J, Chen XY, Zhang H, Xiong LD, Lei H, Deng SH. Hyperparameter optimization for machine learning models based on Bayesian optimization. *J Electron Sci Technol*. 2019;17:26–40.

20. Driessen RS, Bom MJ, van Diemen PA, et al. Incremental prognostic value of hybrid [15O]H_2O positron emission tomography-computed tomography: combining myocardial blood flow, coronary stenosis severity, and high-risk plaque morphology. *Eur Heart J Cardiovasc Imaging*. 2020;21:1105–1113.

21. van Diemen PA, Bom MJ, Driessen RS, et al. Prognostic value of RCA pericoronary adipose tissue CT-attenuation beyond high-risk plaques, plaque volume, and ischemia. *JACC Cardiovasc Imaging*. 2021;14:1598–1610.

22. Fan C, Zhang D. Wald-type rank tests: a GEE approach. *Comput Stat Data Anal*. 2014;74:1–16.

23. Park HB, Heo R, Hartaigh BÓ, et al. Atherosclerotic plaque characteristics by CT angiography identify coronary lesions that cause ischemia: a direct comparison to fractional flow reserve. *JACC Cardiovasc Imaging*. 2015;8:1–10.

24. Gaur S, Øvrehus KA, Dey D, et al. Coronary plaque quantification and fractional flow reserve by coronary computed tomography angiography identify ischaemia-causing lesions. *Eur Heart J*. 2016;37:1220–1227.

25. Ahmadi A, Leipsic J, Øvrehus KA, et al. Lesion-specific and vessel-related determinants of fractional flow reserve beyond coronary artery stenosis. *JACC Cardiovasc Imaging*. 2018;11:521–530.

26. Lin A, van Diemen PA, Motwani M, et al. Machine learning from quantitative coronary computed tomography angiography predicts fractional flow reserve-defined ischemia and impaired myocardial blood flow. *Circ Cardiovasc Imaging*. 2022;15:e014369.

27. De Bruyne B, Hersbach F, Pijls NHJ, et al. Abnormal epicardial coronary resistance in patients with diffuse atherosclerosis but "normal" coronary angiography. *Circulation*. 2001;104:2401–2406.

28. Rizvi A, Hartaigh BÓ, Danad I, et al. Diffuse coronary artery disease among other atherosclerotic plaque characteristics by coronary computed tomography angiography for predicting coronary vessel-specific ischemia by fractional flow reserve. *Atherosclerosis*. 2017;258:145–151.

29. Ahmadi A, Stone GW, Leipsic J, et al. Association of coronary stenosis and plaque morphology with fractional flow reserve and outcomes. *JAMA Cardiol*. 2016;1:350–357.

30. Min JK, Chandrashekhar Y. Atherosclerosis, stenosis, and ischemia: one primary, one secondary, and one tertiary. *JACC Cardiovasc Imaging*. 2018;11:531–533.

31. Nørgaard BL, Leipsic J, Gaur S, et al. Diagnostic performance of noninvasive fractional flow reserve derived from coronary computed tomography angiography in suspected coronary artery disease: the NXT trial (Analysis of Coronary Blood Flow Using CT Angiography: Next Steps). *J Am Coll Cardiol*. 2014;63:1145–1155.

32. Min JK, Leipsic J, Pencina MJ, et al. Diagnostic accuracy of fractional flow reserve from anatomic CT angiography. *JAMA*. 2012;308:1237–1245.

33. Koo BK, Erglis A, Doh JH, et al. Diagnosis of ischemia-causing coronary stenoses by noninvasive fractional flow reserve computed from coronary computed tomographic angiograms: results from the prospective multicenter DISCOVER-FLOW (Diagnosis of Ischemia-Causing Stenoses Obtained Via Noninvasive Fractional Flow Reserve) study. *J Am Coll Cardiol*. 2011;58:1989–1997.

34. van der Bie J, van Straten M, Booij R, et al. Photon-counting CT: review of initial clinical results. *Eur J Radiol*. 2023;163:110829.

35. Lipkin I, Telluri A, Kim Y, et al. Coronary CTA with AI-QCT interpretation: comparison with myocardial perfusion imaging for detection of obstructive stenosis using invasive angiography as reference standard. *Am J Roentgenol*. 2022;219:407–419.

36. Omori H, Matsuo H, Earls J, et al. Abstract 13674: Optimal Hounsfield threshold for lipid-rich plaque by artificial intelligence-enabled quantitative CT using near-infrared spectroscopy. *Circulation*. 2022;146:A13674-A13674.

KEY WORDS artificial intelligence, atherosclerosis, coronary computed tomography angiography, coronary ischemia, stress testing

APPENDIX For supplemental tables, please see the online version of this paper.